

## Lysozyme stability in various deep eutectic solvents using molecular dynamics simulations

Hebbar, Akshatha; Dey, Poulumi; Vatti, Anoop Kishore

**DOI**

[10.1080/07391102.2023.2275178](https://doi.org/10.1080/07391102.2023.2275178)

**Publication date**

2023

**Document Version**

Final published version

**Published in**

Journal of Biomolecular Structure and Dynamics

**Citation (APA)**

Hebbar, A., Dey, P., & Vatti, A. K. (2023). Lysozyme stability in various deep eutectic solvents using molecular dynamics simulations. *Journal of Biomolecular Structure and Dynamics*, 42 (2024)(23), 13325-13333. <https://doi.org/10.1080/07391102.2023.2275178>

**Important note**

To cite this publication, please use the final published version (if applicable). Please check the document version above.

**Copyright**

Other than for strictly personal use, it is not permitted to download, forward or distribute the text or part of it, without the consent of the author(s) and/or copyright holder(s), unless the work is under an open content license such as Creative Commons.

**Takedown policy**

Please contact us and provide details if you believe this document breaches copyrights. We will remove access to the work immediately and investigate your claim.

# Lysozyme stability in various deep eutectic solvents using molecular dynamics simulations

Akshatha Hebbar, Poulumi Dey & Anoop Kishore Vatti

To cite this article: Akshatha Hebbar, Poulumi Dey & Anoop Kishore Vatti (01 Nov 2023): Lysozyme stability in various deep eutectic solvents using molecular dynamics simulations, Journal of Biomolecular Structure and Dynamics, DOI: [10.1080/07391102.2023.2275178](https://doi.org/10.1080/07391102.2023.2275178)

To link to this article: <https://doi.org/10.1080/07391102.2023.2275178>



© 2023 The Author(s). Published by Informa UK Limited, trading as Taylor & Francis Group



View supplementary material [↗](#)



Published online: 01 Nov 2023.



Submit your article to this journal [↗](#)



Article views: 223



View related articles [↗](#)



View Crossmark data [↗](#)

# Lysozyme stability in various deep eutectic solvents using molecular dynamics simulations

Akshatha Hebbar<sup>a</sup> , Poulumi Dey<sup>b</sup> and Anoop Kishore Vatti<sup>a</sup> 

<sup>a</sup>Department of Chemical Engineering, Manipal Institute of Technology (MIT), Manipal Academy of Higher Education (MAHE), Manipal, India;

<sup>b</sup>Department of Materials Science and Engineering, Faculty of Mechanical, Maritime and Materials Engineering (3mE), Delft University of Technology, Delft, Netherlands

Communicated by Ramaswamy H. Sarma

## ABSTRACT

The ability of neat deep eutectic solvents (DESs) to influence protein structure and function has gained considerable interest due to the unstable nature of enzymes or therapeutic proteins, which are often exposed to thermal, chemical, or mechanical stresses when handled at an industrial scale. In this study, we simulated a model globular protein, lysozyme, in water and six choline chloride-based DES using molecular dynamics simulations, to investigate the structural changes in various solvent environments, giving insights into the overall stability of lysozyme. Root mean square deviation (RMSD) and root mean square fluctuations (RMSF) of the C- $\alpha$  backbone indicated that most DESs induced a less flexible and rigid lysozyme structure compared to water. The radius of gyration and end-to-end distance calculations pointed towards higher structural compactness in reline and levuline, while the structure of lysozyme considerably expanded in oxaline. Protein-solvent interactions were further analysed by hydrogen bonding interactions and radial distribution functions (RDF), which indicated a higher degree of lysozyme-hydrogen bond donor (HBD) interactions compared to lysozyme-choline hydrogen bonding. Surface area analysis revealed an overall % increase in total positive, negative, donor, and acceptor surface areas in malicine and oxaline compared to water and other DESs, indicating the exposure of a larger number of residues to interactions with the solvent. Reline, levuline, and polyol-based DESs comparatively stabilized lysozyme, even though changes in the secondary/tertiary structures were observed.

## ARTICLE HISTORY

Received 11 July 2023

Accepted 18 October 2023

## KEYWORDS





Lysozyme; deep eutectic solvents; molecular dynamics simulations; stability; protein-DESs interactions


## 1. Introduction

Deep Eutectic Solvents (DESs) are complexes of a hydrogen bond donor and an acceptor combined in a specific molar ratio to achieve a deep depression in their freezing point, forming homogeneous liquids at room temperature (Smith et al., 2014). DESs are known for a range of favourable characteristics, such as non-volatility, low toxicity, ease of preparation, abundant availability of precursors, chemical stability, and the ability to solvate various molecules (Gurkan et al., 2019; Paiva et al., 2014; Płotka-Wasyłka et al., 2020). DESs are being researched as green solvents in metal finishing (Abbott et al., 2013; Smith, 2013), extraction and synthesis media (Weiz et al., 2016; Zhang et al., 2012), biomass processing (Barbieri et al., 2020; Kumar et al., 2016), gas absorption and solubilization (García et al., 2015), and for handling flow assurance problems in the oil industry (Hu et al., 2021; Sanati et al., 2021). Understanding protein stability, enzymatic activity, and molecular recognition requires a thorough knowledge of conformation and dynamics (Almeida et al., 2022; Kist et al., 2021). DESs provide a suitable environment

for biomolecules and have the potential to be safer alternatives than other solvents. The most recent research and efforts in using DESs are focussed on stabilizing and activating proteins and enzymes. Moreover, it has been reported that pure urea has the ability to induce protein denaturation. However, small-angle neutron scattering (SANS) data revealed that lysozyme maintained its structural integrity when exposed to a ChCl: urea based deep eutectic solvent (DES) (Sanchez-Fernandez et al., 2017). This line of research is gaining prominence due to the emergence of biocatalysts (Bommarius & Paye, 2013; Woodley, 2019) and protein therapeutics (Leader et al., 2008; Liu et al., 2021). Major bottlenecks in protein stability, shelf life, and purification are often encountered during the utilization, formulation and storage at an industrial scale (Pätzold et al., 2019). Since structural stability is closely linked to protein functionality, there is a need to screen efficient, biocompatible, and easily available alternative solvents.

Lysozyme is a 129-residue murein hydrolase belonging to the class of ovo-antimicrobials due to its capability of

**CONTACT** Poulumi Dey  [p.dey@tudelft.nl](mailto:p.dey@tudelft.nl)  Department of Materials Science and Engineering, Faculty of Mechanical, Maritime and Materials Engineering (3mE), Delft University of Technology, Delft, 2628 CD, Netherlands; Anoop Kishore Vatti  [anoop.vatti@manipal.edu](mailto:anoop.vatti@manipal.edu)  Department of Chemical Engineering, Manipal Institute of Technology (MIT), Manipal Academy of Higher Education (MAHE), Manipal, Karnataka, 576104, India.

 Supplemental data for this article can be accessed online at <https://doi.org/10.1080/07391102.2023.2275178>

© 2023 The Author(s). Published by Informa UK Limited, trading as Taylor & Francis Group

This is an Open Access article distributed under the terms of the Creative Commons Attribution-NonCommercial-NoDerivatives License (<http://creativecommons.org/licenses/by-nc-nd/4.0/>), which permits non-commercial re-use, distribution, and reproduction in any medium, provided the original work is properly cited, and is not altered, transformed, or built upon in any way. The terms on which this article has been published allow the posting of the Accepted Manuscript in a repository by the author(s) or with their consent.

hydrolysing peptidoglycan found in bacterial cell walls. It comprises of a single polypeptide chain, constituting two domains and an active cleft, with an overall globular structure stabilised by four disulfide linkages. The active site of lysozyme comprises Glu35 and Asp52. Lysozyme has various applications as natural antimicrobials for food preservation, antibiotics, analgesics, and anti-inflammatory agents, and in the cosmetic industry, making it a commercially important protein (Ercan & Demirci, 2016; Kumari et al., 2020). It has served as a benchmark protein for several early investigations on protein dynamics (Smith & van Gunsteren, 1994), hydrogen bond networks in proteins (Yokomizo et al., 2005), and thermal stability (Meersman et al., 2010) in aqueous media. Esquembre et al. (2013) investigated the effects of pure and hydrated reline and glyceline on the thermal stability, refolding capability, and activity of lysozyme. Normalized fluorescence and far Ultra-Violet (UV) Circular Dichroism (CD) spectra indicated structural compactness and a negligible change in the protein secondary structure in both DESs. However, increasing the temperature led to an irreversible denaturation of lysozyme in reline, and a partially reversible denaturation in glyceline, as the decrease in the mean fluorescence energy was more pronounced in reline compared to glyceline. Folding intermediates dominated by secondary structures were observed at different temperature ranges, with a higher structural compactness in glyceline and buffer compared to reline. The activity of lysozyme in glyceline was severely reduced compared to that in buffer. However, hydration or removal of DES by dialysis facilitated the recovery of the initial structure and activity of the enzyme. Similar results were obtained by Sanchez-Fernandez et al. (2017), who extrapolated data from small-angle nuclear scattering (SANS) to obtain the radius of gyration ( $R_g$ ) of lysozyme in reline and glyceline. While the secondary structures remained relatively unaffected, lysozyme assumed a partially unfolded structure, with  $R_g$  of  $17.2 \pm 0.8$  and  $17.8 \pm 1.0 \text{ \AA}$  in glyceline and reline, respectively. The reduction in enzyme activity was attributed to the high viscosity of both DESs and a change in the lysozyme conformation in the DESs compared to buffer.

Sanchez-Fernandez et al. (2022) studied the effect of hydrated reline and glyceline on the structure and stability of lysozyme, along with immunoglobulin, and bovine serum albumin (BSA). UV-visible, SANS, and far UV CD spectra revealed a non-monotonic change in the conformations of each protein when exposed to DESs in increasing water concentrations. At lower water concentrations, water displaced chloride ions, promoting solvent-protein interactions that caused a partial unfolding of the protein. Higher water concentrations disrupted the hydrogen bonding network of the DES and caused water to preferentially solvate the protein instead of the DES. Lysozyme recovered its tertiary structure completely after rehydrating the neat DES. The study concluded that the level of hydration and subsequent protein-solvent interactions also govern protein folding to a great extent. Sanchez Fernandez et al. (2022) also reported the ability of pure glyceline to store high concentrations of lysozyme. UV-Visible and SANS spectra of lysozyme/glyceline systems with varying lysozyme concentrations (4–143 mg/mL) indicated that the protein retained its globular nature

without aggregating. However, a change in the secondary and tertiary structures in dilute and concentrated systems was observed. The solubility of lysozyme in glyceline (143 mg/mL) was greater than that in aqueous saline buffers and pure glycerol. The study also proved the ability of glyceline to preserve lysozyme (28 mg/mL) at room temperature (20 °C) for 40 days, after which it was successfully recovered by extensive dialysis or hydration with a negligible deterioration in its structure and activity.

Belviso et al. (2021) performed the experimental investigations using high-resolution X-ray diffraction to probe the DES component's interactions with lysozyme residues. It was concluded that Choline ions strongly interact with residues Trp62 and Trp123 of lysozyme. Besides protein stability studies, the role of carboxylic acid-based DESs in the crystallization and extraction of lysozyme have also been investigated (Belviso et al., 2021; Xu et al., 2019) which could significantly cut down protein purification and production costs. Lysozyme fibrillation in carboxylic acid-based DESs has been studied to aid the synthesis of potential nanomaterials (Silva et al., 2018). Although experimental studies provide insights into the structure and dynamics of proteins in DESs down to the secondary structure level, analysis of protein-solvent interactions at a molecular level using molecular dynamics (MD) simulations gives us further insights into protein stability. Several MD simulation studies have been performed to investigate the effects of neat or hydrated DESs, mainly reline, glyceline, and ethaline, on the structure and stability of lipase (Kovács et al., 2022; Monhemi et al., 2014; Shehata et al., 2020), alcohol dehydrogenase (Bittner et al., 2021, 2022), lysozyme (Kumari et al., 2020), BSA (Kumari et al., 2022), and other small proteins (Pal et al., 2020; Sarkar et al., 2017).

Kumari et al. (2020) analysed the structural changes in lysozyme in neat and hydrated reline using root mean square deviation (RMSD), root mean square fluctuations (RMSF),  $R_g$ , and hydrogen bond analysis. The C- $\alpha$  backbone of the protein underwent an initial shift in conformation in neat reline, which remained unchanged for the rest of the simulation. In contrast, increased RMSD and RMSF meant more drastic conformational changes observed in 50/50 reline/water mixtures. Lysozyme in pure reline had the highest solvent accessible surface area (SASA) and  $R_g$ , indicating a partial unfolding of the protein structure due to the replacement of ordered helical coils with unordered bends that left certain buried residues exposed to the solvent. However, the structure was rigid and stable compared to its native form in water. Reline-protein interactions were characterized by hydrogen bonds, dominated by protein-choline, which decreased upon adding water.

In a recent study conducted by Parisse et al. (2023) the force field parameters of pure DES were calibrated through the measurement of pair distribution functions. Furthermore, the stability of lysozyme in mixtures of aqueous glyceline was evaluated. The research conducted in this study introduced an alternative approach to assess protein flexibility through the computation of a dynamic cross-correlation matrix (DCCM) for atomic displacements. The experimental findings revealed that the presence of DES led to a reduction in the correlated motion of lysozyme's atoms within its

backbone. This observation indicates an increase in the rigidity of the protein's structure. Nevertheless, the functional properties of lysozyme were not negatively impacted by the DES, as evident from the continued presence of characteristic fluctuations associated with its function. The findings of the study indicated that the RMSF, RMSD, and radius of gyration values were consistent across all three force fields used to analyze the properties of the DES.

Recent research has highlighted the growing importance of DESs in protein storage and stability. However, the interaction between DESs and lysozyme at the molecular level has only been investigated in a limited number of studies. Although previous studies have investigated the interactions between lysozyme and a limited number of deep eutectic solvents (DESs) (Yadav & Venkatesu, 2022), there is a necessity to broaden the range of DESs examined by molecular dynamics (MD) simulations, extending beyond reline and glyceline. This work aims to examine the impact of six distinct choline chloride-based DESs as shown in Table 1—reline, glyceline, ethaline, levuline, malicine, and oxaline—on the structure and stability of lysozyme using MD simulations. The selection of DESs was based on their representation of three distinct categories of hydrogen bond donors (HBDs), specifically amides, polyols, and carboxylic acids. This choice was made to provide a comparative analysis of their respective interactions with lysozyme and the resulting effects. The structural, dynamic, and protein-solvent interactions within each system were comprehensively examined through the computation of various metrics, including RMSD, RMSF,  $R_g$ , end-to-end distance, radial distribution function (RDF), surface area, and hydrogen bond analysis. The MD simulations over a simulation period of 120 ns were analyzed, and the obtained results were subsequently compared to those observed in the protein-water system.

## 2. Computational details

MD simulations were carried out using Desmond MD code (Bowers et al., 2006) within the Schrödinger simulation software (Release, 2021). The 3D structure of lysozyme without

**Table 1.** Deep eutectic solvents contain specific molar ratios of different hydrogen bond donors (HBD) and choline chloride (ChCl).

HBD	Molar ratios	Name of DES
Urea	1:2	Reline
Glycerol	1:2	Glyceline
Ethylene glycol	1:2	Ethaline
Levulinic acid	1:2	Levuline
Malic acid	1:1	Malicine
Oxalic acid	1:1	Oxaline

ligands was imported from the Protein Data Bank (PDB ID: 1AKI) with a resolution of 1.5 Å. Protein preparation was employed to process the protein structure before building the systems. Chemical Component Dictionary (CCD) was used to assign bond orders. Selenomethionines, which are often experimentally used to ease protein crystallisation, were converted to methionines. In addition, disulphide bonds were created, waters beyond 3 Å from heteroatom groups were removed, and hydrogen bond assignment was refined based on sample water orientations at a pH of 7. Restrained minimisation was conducted to converge all heavy atoms to RMSD within 0.3 Å using the latest Optimised Parameters for Liquid Simulations (OPLS4) (Lu et al., 2021) force fields.

The minimized protein was solvated in water using the Single Point Charge (SPC) water model, and a cubic simulation box having dimensions of 70 Å. Eight Cl<sup>-</sup> ions were added to the system to neutralise the positive charges on lysozyme. Lysozyme-DES systems were built using the structures of the hydrogen-bond acceptor (HBA), choline chloride ([Ch<sup>+</sup>][Cl<sup>-</sup>]), and different hydrogen-bond donors (HBDs) for each DES (urea, glycerol, ethylene glycol, levulinic acid, malic acid, and oxalic acid). One lysozyme molecule was solvated in [Ch<sup>+</sup>][Cl<sup>-</sup>] and the respective HBD in their eutectic molar ratios. The number of solvent molecules and the dimensions of the simulation box of each system are tabulated in Table 2. A cubic simulation box was considered in all cases. While the DESs in this study are being referred using different names, it should be noted that they represent binary eutectic mixtures of respective HBA and HBDs, and not unique compounds (Bittner et al., 2021).

The solvent molecules were explicitly defined to simulate a bulk solvent environment and to identify protein-solvent interactions. The current OPLS4 force field has shown great promise in understanding protein folding and for accurate prediction of protein reorganization free energy to predict binding free energies for ligands accurately (Fajer et al., 2023). In this work, OPLS4 force fields were used to describe the bonded and non-bonded potentials of each DES to describe the properties of DESs (Doherty & Acevedo, 2018; Maity et al., 2020; Salehi et al., 2019; Sarkar et al., 2017). Particle mesh Ewald summations were used to sum up long-range interactions over the periodic images, requiring the system to be electrically neutral. Hence, 8 chloride ions were added to each system (Frenkel & Smit, 2002). For the simulation run, firstly, a relaxation protocol was applied, consisting of a 20 ps NVT Brownian minimisation at 10 K, followed by a 20 ps NPT Brownian minimisation at 100 K, ending with a

**Table 2.** Number of molecules of solvent considered for each system, along with simulation box dimensions (one molecule of lysozyme was incorporated into each system, with eight additional Cl<sup>-</sup> ions for neutralization.).

System (molar ratios)	Name of DES	Water	Choline (Ch <sup>+</sup> )	Chloride (Cl <sup>-</sup> )	HBD	Simulation box size (Å <sup>3</sup> )
Lysozyme-water	-	10,438	-	-	-	70.059 × 67.881 × 71.012
Lysozyme-ChCl/urea (1:2)	Reline	-	1000	1000	2000	71.598 × 70.648 × 75.731
Lysozyme-ChCl/glycerol (1:2)	Glyceline	-	1000	1000	2000	78.856 × 74.421 × 72.997
Lysozyme-ChCl/ethylene glycol (1:2)	Ethaline	-	1000	1000	2000	78.031 × 78.758 × 79.99
Lysozyme-ChCl/levulinic acid (1:2)	Levuline	-	1000	1000	2000	83.512 × 83.024 × 82.502
Lysozyme-ChCl/malic acid (1:1)	Malicine	-	1333	1333	1333	81.230 × 80.313 × 81.447
Lysozyme-ChCl/oxalic acid (1:1)	Oxaline	-	1333	1333	1333	75.388 × 77.222 × 77.841



100 ps NPT MD stage at 100 K. Brownian minimisation was again run for 100 ps. A 40 ns NPT equilibration run at 1.01325 bar was carried out, followed by an NVT production run for 120 ns. The temperature for the production run was set to 300 K to simulate room temperature, and a time step of 2 fs was considered. Nose Hoover thermostat with a relaxation time of 1 ps and Martyna Tobias-Klein barostat (isotropic coupling) with a relaxation time of 2 ps were used. A cut-off radius of 9 Å was chosen for Coulombic interactions.

### 3. Results and discussion

#### 3.1. Protein structures in water and various DESs

Figure S1 shows the final tertiary structure of lysozyme in water. Secondary structures are represented in various colours in the figure. Further, the final lysozyme structures in six DESs studied, are shown in Figure S2. Reline is observed to induce a compact structure form of lysozyme, which indicates a change in its overall tertiary structure. While lysozyme maintains a slightly unfolded structure in glyceline, a certain degree of expansion is observed compared to reline. The structures of the protein in ethaline and levuline are comparable to that in water. Further, elongation in the lysozyme structure is observed in malicine. Lysozyme in oxaline, on the other hand, is in the form of an unfolded structure.

#### 3.2. Root mean square deviation (RMSD)

The RMSD of C- $\alpha$  atoms of lysozyme provides a measure of the average structural deviations in its backbone with simulation time compared to a reference frame. The RMSD of frame  $x$  is calculated using the following equation:

$$RMSD_x = \sqrt{\frac{1}{N} \sum_i^N (r'_i(t_x) - r_i(t_{ref}))^2} \quad (1)$$

where  $r_i$  and  $N$  are the  $i$ th and total number of C- $\alpha$  atoms, respectively. The position of atom  $i$  at time  $t_x$  is superposed over its position at the reference time  $t_{ref}$  to get position  $r'_i$ . The square of the relative displacements in the atom is summed over all the  $N$  selected atoms in each frame and averaged out. This procedure is repeated for all the frames in the trajectory.

Figure 1 represents the RMSD of lysozyme in all seven systems, represented as a moving average over 100 data points to reduce noise and visualize data effectively. Frame 0 was considered as the reference frame in all cases. RMSD values underwent a steady rise, which ultimately stabilised around a thermal average of around 0.75 Å towards the end of the simulation (after 90 ns) for most DES systems except glyceline and oxaline, where the C- $\alpha$  deviations increased steadily from 0.5 Å in the beginning, to 1.25 and 1 Å, respectively even at the end of the simulation. However, the deviations in all seven systems were within 1–3 Å.

The RMSD magnitudes of lysozyme in water are often greater compared to the majority of DESs, with fluctuations observed around 1.25 Å. It suggests that the lysozyme exhibits reduced structural stability in an aqueous environment

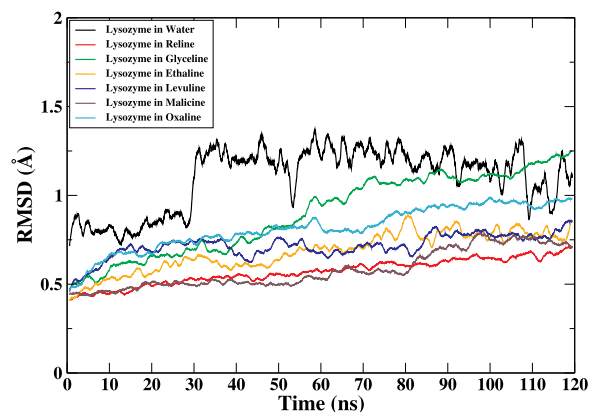


Figure 1. Root mean square deviations of lysozyme in water (black), reline (red), glyceline (green), ethaline (orange), levuline (blue), malicine (maroon), and oxaline (turquoise) over the entire simulation time of 120 ns.

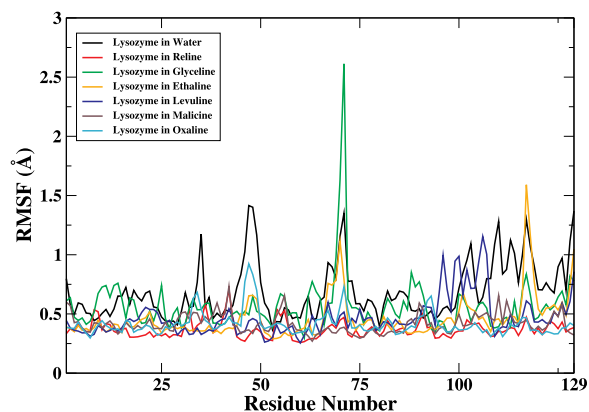


Figure 2. Root mean square fluctuations of lysozyme residues in various solvent media. Colour scheme is as follows: Water in black, reline in red, glyceline in green, ethaline in orange, levuline in blue, malicine in maroon, and oxaline in turquoise.

when compared to a DES medium. While this deviates from the findings of Kumari et al. (Kumari et al., 2020), which revealed that lysozyme had a larger RMSD value in reline compared to water, their study also found that RMSD variations were less pronounced in reline. The observed phenomenon was attributed to a decrease in local protein dynamics, which can be related to an increase in solvent viscosity. The findings of the present study demonstrate that the presence of lysozyme in reline resulted in the lowest RMSD value, suggesting that it imparted the highest degree of backbone rigidity when compared to alternative solvents.

#### 3.3. Root mean square fluctuations (RMSF)

RMSF provides crucial insights on the local flexibility of every protein residue, averaged over the simulation time  $t$  as shown in the following equation:

$$RMSF_i = \sqrt{\langle (R_i - \langle R_i \rangle)^2 \rangle} \quad (2)$$

Where  $R_i$  is the position vector of atom  $i$  and the angled brackets represent the time average over the entire MD run. Figure 2 represents the RMSF of all the 129 residues of lysozyme in water and six DESs, taken with respect to the C- $\alpha$  atoms of each residue. The peaks indicate the residues

undergoing the highest number of fluctuations during the simulation. Higher fluctuations are generally expected at the terminals (unless the ends of the protein are capped during preparation) and at bends, while regions having  $\alpha$ -helix and  $\beta$ -sheet secondary structures are stabilised by hydrogen bonding and tend to show limited mobility.

Three areas of highest flexibility were observed around the active site region (residues 35–52), bend regions in Domain II (residues 54–79), and the C-terminal region. The flexibility of the active site region is the highest for lysozyme in water, followed by oxaline. However, the overall fluctuations around the active site are subdued in the DESs compared to water, with reline, levuline, and malicine showing the least RMSF of 0.3 Å from residues 45–52. Ethaline and glyceline induce weak peak fluctuations in this range. Glyceline induced a drastic fluctuation of residue 70, reaching a value of around 2.5 Å, followed by water and ethaline. This is also reflected in the RMSD results, where the lysozyme backbone undergoes increased deviations in glyceline. Similar fluctuations at the turn around the 119th residue were observed in ethaline, followed by water.

The urea and carboxylic acid based DESs tend to suppress bend movements to a greater extent, which could be attributed to a higher solvent viscosity. Fluctuations in the  $\alpha$ -helix region (around the 100th residue) were significantly lower in all DESs except levuline, where peak intensities were comparable to those in water. Overall, the average RMSF of the protein backbone is lower in most DES media compared to water, indicating an increase in structural rigidity, and is supported by the RMSD results. The RMSF observed in our study for the C- $\alpha$  atoms are consistent with the findings reported in a recent study conducted by Parisse et al. (2023). For the majority of residues, RMSF exhibits a range that is below 0.15 nm. Significant alterations in the RMSF are observed specifically at residue 70. The findings of our study indicate a range in the RMSF,  $\sim$ 0.25 nm. Additionally, it should be noted that our simulations exclusively used pure glyceline DES, whereas Parisse et al. (2023) employed a mixture of glyceline and water (80:20 w/w).

### 3.4. Radius of gyration ( $R_g$ ) and end-to-end distance

While protein compactness has been defined as the ratio of its accessible surface area to the spherical surface area occupying the same volume as the protein, Lobanov et al. (2008) correlated the folding rate and structural compactness of proteins to their radius of gyration, which assumes a different range of values for various classes of proteins, according to their secondary structures. Radius of gyration ( $R_g$ ) is calculated using the following equation:

$$R_g = \sqrt{\frac{\sum_i r_i^2 m_i}{\sum_i m_i}} \quad (3)$$

where  $r_i$  is the position of atom  $i$  with respect to the center of the molecule and  $m_i$  is the mass of atom  $i$ . The changes in  $R_g$  throughout the simulation time for the six DES systems are shown in Figure 3(a), with the corresponding values obtained in water for comparison. Moving averages have

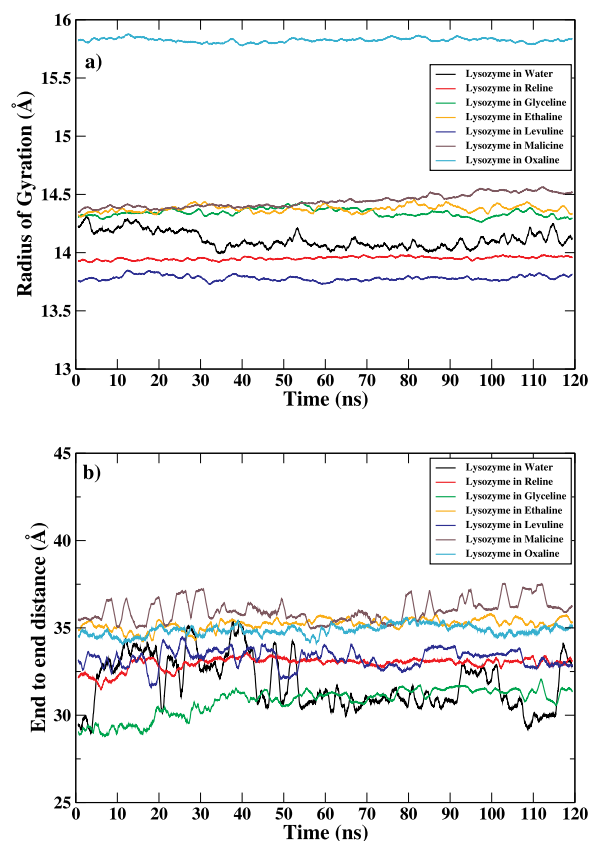


**Figure 3.** (a) Radius of gyration and (b) end-to-end distances of lysozyme in various solvent media. Colour scheme is as follows: Water in black, reline in red, glyceline in green, ethaline in orange, levuline in blue, malicine in maroon, and oxaline in turquoise.

**Table 3.** Mean radius of gyration and time series standard deviation of lysozyme in various solvent media (all measurements in Å).

Solvent	Mean radius of gyration	Time series standard deviation
Water	14.11	0.097
Reline	13.95	0.030
Glyceline	14.34	0.044
Ethaline	14.37	0.044
Levuline	13.78	0.037
Malicine	14.44	0.064
Oxaline	15.82	0.037

been applied over 100 data points. The mean  $R_g$  and time series standard deviation over 120 ns of simulation time for all systems are tabulated in Table 3. The radius of gyration of lysozyme in water is obtained as 14.25 Å, which stabilized to 14.11 Å after 40 ns. This agrees with the values obtained in the literature (Kumari et al., 2020).  $R_g$  in reline is slightly lower than that in water, with a difference of 0.16 Å, indicating that the structure of lysozyme has become more compact. This was also seen in the 3D protein structure in reline (Figure S1(b)). However, the absolute value (13.95 Å) deviates from that of the experimentally obtained value of 17.8 Å (Sanchez-Fernandez et al., 2017) and 16.5 Å obtained in MD simulations (Kumari et al., 2020), which could be attributed to differences in force field parameters adopted in this study in comparison to the findings of Kumari et al. (2020). OPLS4 force fields showed the highest decrease in lysozyme ' $R_g$ ' among all systems in comparison to water with levuline.

The  $R_g$  of lysozyme in glyceline and ethaline stabilized at 14.3 Å, which was slightly higher than that in water, suggesting an expanded globular structure. This is consistent with the RMSF results, which hinted at considerable fluctuations in the bend regions. The most significant increase in  $R_g$  was observed for lysozyme in oxaline, with an average value of 15.82 Å, indicating that the protein has significantly expanded and undergone a relatively drastic change in its secondary structure, as indicated in Figure S1(g).

The dynamics of various biomolecules like DNA and certain proteins can be obtained by modelling them as semi-flexible chains (Cifra et al., 2008), using the worm-like chain model. This models a semi-flexible chain by dividing it into  $N$  segments of a fixed length  $L_0$ . Three parameters are defined: the end-to-end distance, which is the distance between one end of a chain to the other end, the extended chain length, the distance between the ends of a fully extended chain; and the persistence length, the distance beyond which the molecule chain has greater flexibility at equilibrium. The mean squared end-to-end distance, is defined by the following equation (Zhang et al., 2019; Brinkers et al., 2009):

$$\langle h^2 \rangle = 2L_p L_0 [1 - (L_p/L_0)(1 - \exp(-L_0/L_p))] \quad (4)$$

where  $\langle h^2 \rangle$  is the mean squared end-to-end distance,  $L_0$  is the extended chain length and  $L_p$  is the persistence length. The average end-to-end distances, extended chain, and persistence lengths of lysozyme in each solvent system are tabulated in Table 4. The end-to-end distance as a function of simulation time for each system is depicted as moving averages over 100 data points in Figure 3(b). All systems show a near constant extended chain length of around 214 Å, which is several orders of magnitude larger than the average persistence length (2 Å), indicating that lysozyme is a flexible protein, due to its globular nature (Gerrits et al., 2021).

The lysine (LYS1) and leucine (LEU129) are the first and last amino acids in the lysozyme polypeptide chain. LYS1 and LEU129 lie in Domain I of lysozyme, both are part of flexible bend regions. The average end-to-end distance was 31.823 Å in water, which kept undergoing drastic fluctuations throughout the simulation time. This was also depicted in the RMSF result of the C-terminal. The end-to-end distance in glyceline stabilised to a value comparable to that in water after 50 ns. Reline and ethaline induced least fluctuations in the end-to-end distances, indicating a rigid domain structure, however, the residue distance was greater in ethaline. While the end-to-end distances of lysozyme in ethaline and oxaline were comparable,  $R_g$  results indicate a more expanded

structure in oxaline, indicating that the major secondary structural changes have occurred in other regions of the protein. Malicine recorded the highest and most fluctuating end-to-end distance of lysozyme amongst all DESs, suggesting a disruption in the structure of domain I, leading to an increase in the residue distances, as also shown by the calculated  $R_g$  value of 14.44 Å.

### 3.5. Hydrogen bonds

A hydrogen bond between a donor and an acceptor atom is assigned when the distance between them is within 2.5 Å and the angle between them (donor atom—hydrogen atom—acceptor atom) is within 45°. Hydrogen bonding governs intra-protein and protein-solvent interactions, and, in the case of DESs, HBA-HBD interactions as well, and can be instrumental in understanding how the interactions in the system change in various DESs (Pal et al., 2020; Sarkar et al., 2017). Table 5 outlines the average number of protein-protein hydrogen bonds in each system, along with protein-choline, protein-HBD, and protein-water interactions, the absolute numbers normalized according to the number of species present in the system for comparison. The number of hydrogen bonds within lysozyme fluctuated around an average value in all DESs throughout the simulation time. Levuline and ethaline supported the formation of maximum intra-protein hydrogen bonds, followed by reline and malicine, where the hydrogen bonding interactions were comparable to that in water. A higher number of lysozyme-HBD interactions were observed compared to lysozyme-choline interactions for all DES systems, higher than the average number of lysozyme-water interactions, indicating that the DESs indeed have a significant effect on the structure of the protein. Similar results were observed in a study by Belviso et al. (2021), where an analysis of the protein crystal structure with the DES showed choline undergoing strong interactions with the Trp62 and Trp123 residues of lysozyme. Four major binding sites were observed between urea and residues at different regions of the protein, indicating significant HBD-protein interactions.

Glyceline and malicine showed the highest number of lysozyme-glycerol and lysozyme-malic acid interactions, which could be attributed to a greater number of hydrogen bond donating functional groups compared to the other HBDs. Glyceline and oxaline also induced a sharp decrease in intra-protein interactions, and an increase in lysozyme-choline hydrogen bonds, indicating a change in the overall protein conformation, however, the effects were markedly

**Table 4.** Average end-to-end distances, persistence length, and time series standard deviation of lysozyme in various solvent media.

Mixture	End-to-end distance (Å)	Time series standard deviation (Å)	Persistence length (Å)
Water	31.823	1.817	2.392
Reline	32.968	0.607	2.568
Glyceline	30.780	0.930	2.212
Ethaline	35.222	0.491	2.938
Levuline	33.259	0.768	2.616
Malicine	36.004	0.784	3.101
Oxaline	34.863	0.760	2.871

**Table 5.** Number of hydrogen bonds in various solvent media for protein-protein, protein-choline, protein-HBD, and protein-water normalized to the number of choline, HBD, and water molecules in the system.

Mixture	Protein-protein	Protein-choline	Protein-HBD	Protein-water
Water	120	–	–	0.024
Reline	125	0.017	0.045	–
Glyceline	97	0.014	0.050	–
Ethaline	130	0.005	0.047	–
Levuline	145	0.004	0.046	–
Malicine	127	0.012	0.052	–
Oxaline	80	0.012	0.047	–



different. While lysozyme in glyceline showed higher RMSD and RMSF values, the overall  $R_g$  remained at 14.3 Å, showing smaller changes in secondary structure compared to oxaline, where the  $R_g$  increased to 15.8 Å. Figures S1(c,g) also support these observations, where lysozyme in oxaline shows an expanded structure compared to that in glyceline. The number of lysozyme-choline hydrogen bonds in oxaline steadily increases towards the end of the simulation time, hinting at interactions with the exposed tryptophan residues (Belviso et al., 2021; Sanchez-Fernandez et al., 2022). Overall, the nature of the HBD also plays a crucial role in protein structure, supported by earlier observations of neat DESs, such as glyceline forming a protective hydration layer around lysozyme, thus retaining its globular nature and backbone rigidity, even though a change in the secondary structure is seen (Sanchez-Fernandez et al., 2022). Further, RDF for the following pairs: lysozyme – HBD, lysozyme – choline, and lysozyme – chloride is discussed in Supplemental Data (Figure S3).

### 3.6. Surface areas

An analysis of the protein surface provided insights into its extent of folding and the relative distributions of charges, hydrophobic groups, total donor, and acceptor residues present on its surface. Hence, we can predict the extent of protein-solvent or protein-ligand interactions, or protein aggregation (Belviso et al., 2021). The total surface area, sum positive, sum negative, total donor, and total acceptor surface areas were calculated for each system and the percentage relative deviations in each DES with respect to the corresponding surface areas in water were found out, as shown in Figure 4.

All DES systems showed an increase in the total lysozyme surface areas compared to water, with levuline and malicine reporting a higher increase compared to other DES systems. Reline, ethaline, and glyceline were the only DESs to show some degree of variations in the distribution of residues having a positive potential at the protein surface compared to water, while lysozyme in all DESs underwent significant variations in the distribution of negative, donor, and acceptor residues on its surface. A decrease in certain types of surface residues seen in the first four systems indicates a possible rearrangement of the secondary structure, and an increase in the protein structural compactness compared to water. The highest increase in both donor and acceptor groups with

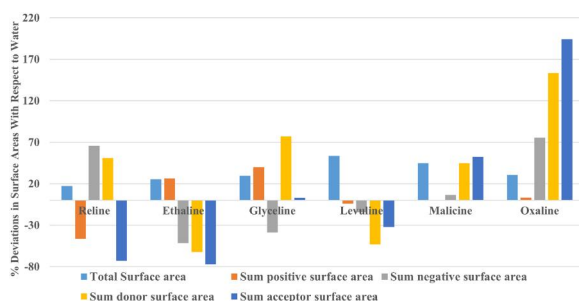


**Figure 4.** Percentage deviations of total surface area, sum positive, sum negative, sum donor, and sum acceptor surface areas of lysozyme in all six DES systems, with water as the reference solvent.

respect to water was seen in malicine and oxaline, which can be attributed to a partial unfolding of the structure, exposing more protein residues to interact with surrounding molecules. This also increases the aggregation propensity of lysozyme within such solvents, as experimentally observed in certain COOH-based DESs (Silva et al., 2018).

## 4. Conclusions

The focus of this investigation was to examine the impact of water and six distinct choline chloride-based deep eutectic solvents (DESs) containing urea, glycerol, ethylene glycol, levulinic acid, malic acid, and oxalic acid as their hydrogen bond donors (HBDs) on the structure and conformation of lysozyme. This was achieved using the molecular dynamics (MD) simulations. The analysis of root-mean-square deviation (RMSD) and root-mean-square fluctuation (RMSF) indicated a notable reduction in the flexibility of the backbone in the majority of DES systems when compared to water. The structure of levuline and reline exhibited greater compactness compared to water, while the presence of oxaline significantly increased the  $R_g$  value. The lysozyme structure was comparatively flexible in glyceline and ethaline. These results were substantiated by the 3D protein structures obtained towards the end of the simulation. Hydrogen bond analysis showed more lysozyme—HBD, followed by lysozyme—chloride interactions. While both glyceline and oxaline showed a decrease in intra-protein hydrogen bonding, oxaline induced a drastic change in the overall conformation of lysozyme, expanding its structure. In contrast, glyceline seemed to retain its globular nature even though fluctuations in the bend regions were observed. Malicine and oxaline also caused a substantial increase in the distribution of the total negative, donor, and acceptor residues on the protein surface compared to water, indicating a probable exposure of buried residues to the surrounding environment. Further refinement of force field parameters and experimental validation of these results can provide additional insights into the role of neat DESs as protein storage and stabilisation media.

## Acknowledgements

Anoop Kishore Vatti would like to thank Schrödinger Centre for Molecular Simulations, MAHE, Manipal for their support.

## Disclosure statement

No potential conflict of interest was reported by the author(s).

## Funding

The author(s) reported there is no funding associated with the work featured in this article.

## ORCID

Akshatha Hebbar  <http://orcid.org/0000-0002-5445-7925>

Anoop Kishore Vatti  <http://orcid.org/0000-0003-3023-3684>

## References

- Abbott, A. P., Frisch, G., & Ryder, K. S. (2013). Electroplating using ionic liquids. *Annual Review of Materials Research*, 43(1), 335–358. <https://doi.org/10.1146/annurev-matsci-071312-121640>
- Almeida, J. S., Capela, E. V., Loureiro, A. M., Tavares, A. P. M., & Freire, M. G. (2022). An overview on the recent advances in alternative solvents as stabilizers of proteins and enzymes. *ChemEngineering*, 6(4), 51. <https://doi.org/10.3390/chemengineering6040051>
- Barbieri, J. B., Goltz, C., Batistão Cavalheiro, F., Theodoro Toci, A., Igarashi-Mafra, L., & Mafra, M. R. (2020). Deep eutectic solvents applied in the extraction and stabilization of rosemary (*Rosmarinus officinalis* L.) phenolic compounds. *Industrial Crops and Products*, 144, 112049. <https://doi.org/10.1016/j.indcrop.2019.112049>
- Belviso, B. D., Perna, F. M., Carrozzini, B., Trotta, M., Capriati, V., & Caliandro, R. (2021). Introducing protein crystallization in hydrated deep eutectic solvents. *ACS Sustainable Chemistry & Engineering*, 9(25), 8435–8449. <https://doi.org/10.1021/acssuschemeng.1c01230>
- Bittner, J. P., Huang, L., Zhang, N., Kara, S., & Jakobtorweihen, S. (2021). Comparison and validation of force fields for deep eutectic solvents in combination with water and alcohol dehydrogenase. *Journal of Chemical Theory and Computation*, 17(8), 5322–5341. <https://doi.org/10.1021/acs.jctc.1c00274>
- Bittner, J. P., Zhang, N., Huang, L., Domínguez de María, P., Jakobtorweihen, S., & Kara, S. (2022). Impact of deep eutectic solvents (DESs) and individual des components on alcohol dehydrogenase catalysis: Connecting experimental data and molecular dynamics simulations. *Green Chemistry*, 24(3), 1120–1131. <https://doi.org/10.1039/D1GC04059F>
- Bommarius, A. S., & Paye, M. F. (2013). Stabilizing biocatalysts. *Chemical Society Reviews*, 42(15), 6534–6565. <https://doi.org/10.1039/C3CS60137D>
- Bowers, K. J., Chow, E., & Xu, H. (2006). Molecular dynamics simulations on commodity clusters. In *Proceedings of the 2006 ACM IEEE Conference on Supercomputing, SC 06*. ACM. <https://doi.org/10.1145/1188455.1188544>
- Brinkers, S., Dietrich, H. R. C., de Groote, F. H., Young, I. T., & Rieger, B. (2009). The persistence length of double stranded DNA determined using dark field tethered particle motion. *The Journal of Chemical Physics*, 130(21), 215105. <https://doi.org/10.1063/1.3142699>
- Cifra, P., Benkova, Z., & Bleha, T. (2008). Persistence lengths and structure factors of wormlike polymers under confinement. *The Journal of Physical Chemistry. B*, 112(5), 1367–1375. <https://doi.org/10.1021/jp076355n>
- Doherty, B., & Acevedo, O. (2018). Opls force field for choline chloride-based deep eutectic solvents. *The Journal of Physical Chemistry. B*, 122(43), 9982–9993. <https://doi.org/10.1021/acs.jpccb.8b06647>
- Ercan, D., & Demirci, A. (2016). Recent advances for the production and recovery methods of lysozyme. *Critical Reviews in Biotechnology*, 36(6), 1078–1088. <https://doi.org/10.3109/07388551.2015.1084263>
- Esquembre, R., Sanz, J. M., Wall, J. G., del Monte, F., Mateo, C. R., & Ferrer, M. L. (2013). Thermal unfolding and refolding of lysozyme in deep eutectic solvents and their aqueous dilutions. *Physical Chemistry Chemical Physics*, 15(27), 11248–11256. <https://doi.org/10.1039/C3CP44299C>
- Fajer, M., Borrelli, K., Abel, R., & Wang, L. (2023). Quantitatively accounting for protein reorganization in computer-aided drug design. *Journal of Chemical Theory and Computation*, 19(11), 3080–3090. <https://doi.org/10.1021/acs.jctc.3c00009>
- Frenkel, D., & Smit, B. (2002). Chapter 12 – Long-range interactions. In D. Frenkel & B. Smit (Eds.), *Understanding molecular simulation* (2nd ed., pp. 291–320). Academic Press. Retrieved from: <https://www.sciencedirect.com/science/article/pii/B9780122673511500146>
- García, G., Aparicio, S., Ullah, R., & Atilhan, M. (2015). Deep eutectic solvents: Physicochemical properties and gas separation applications. *Energy & Fuels*, 29(4), 2616–2644. <https://doi.org/10.1021/ef5028873>
- Gerrits, L., Hammink, R., & Kouwer, P. H. J. (2021). Semiflexible polymer scaffolds: An overview of conjugation strategies. *Polymer Chemistry*, 12(10), 1362–1392. <https://doi.org/10.1039/D0PY01662D>
- Gurkan, B., Squire, H., & Pentzer, E. (2019). Metal-free deep eutectic solvents: Preparation, physical properties, and significance. *The Journal of Physical Chemistry Letters*, 10(24), 7956–7964. <https://doi.org/10.1021/acs.jpcclett.9b01980>
- Hu, C., Fu, S., Zhu, L., Dang, W., & Zhang, T. (2021). Evaluation and prediction on the effect of ionic properties of solvent extraction performance of oily sludge using machine learning. *Molecules*, 26(24), 7551. <https://doi.org/10.3390/molecules26247551>
- Kist, J. A., Zhao, H., Mitchell-Koch, K. R., & Baker, G. A. (2021). The study and application of biomolecules in deep eutectic solvents. *Journal of Materials Chemistry. B*, 9(3), 536–566. <https://doi.org/10.1039/D0TB01656J>
- Kovács, A., Yusupov, M., Cornet, I., Billen, P., & Neyts, E. C. (2022). Effect of natural deep eutectic solvents of non-eutectic compositions on enzyme stability. *Journal of Molecular Liquids*, 366, 120180. <https://doi.org/10.1016/j.molliq.2022.120180>
- Kumar, A. K., Parikh, B. S., & Pravakar, M. (2016). Natural deep eutectic solvent mediated pretreatment of rice straw: Bioanalytical characterization of lignin extract and enzymatic hydrolysis of pretreated biomass residue. *Environmental Science and Pollution Research International*, 23(10), 9265–9275. <https://doi.org/10.1007/s11356-015-4780-4>
- Kumari, M., Kumari, P., & Kashyap, H. K. (2022). Structural adaptations in the bovine serum albumin protein in archetypal deep eutectic solvent reline and its aqueous mixtures. *Physical Chemistry Chemical Physics*, 24(9), 5627–5637. <https://doi.org/10.1039/D1CP05829K>
- Kumari, P., Kumari, M., & Kashyap, H. K. (2020). How pure and hydrated reline deep eutectic solvents affect the conformation and stability of lysozyme: Insights from atomistic molecular dynamics simulations. *The Journal of Physical Chemistry. B*, 124(52), 11919–11927. <https://doi.org/10.1021/acs.jpccb.0c09873>
- Leader, B., Baca, Q. J., & Golan, D. E. (2008, January). Protein therapeutics: A summary and pharmacological classification. *Nature Reviews. Drug Discovery*, 7(1), 21–39. <https://doi.org/10.1038/nrd2399>
- Liu, J., Ting, J. P., Al-Azzam, S., Ding, Y., & Afshar, S. (2021). Therapeutic advances in diabetes, autoimmune, and neurological diseases. *International Journal of Molecular Sciences*, 22(6), 2805. <https://doi.org/10.3390/ijms22062805>
- Lobanov, M., Bogatyreva, N., & Galzitskaya, O. (2008). Radius of gyration as an indicator of protein structure compactness. *Molecular Biology*, 42(4), 623–628. <https://doi.org/10.1134/S0026893308040195>
- Lu, C., Wu, C., Ghoreishi, D., Chen, W., Wang, L., Damm, W., Ross, G. A., Dahlgren, M. K., Russell, E., Von Bargen, C. D., Abel, R., Friesner, R. A., & Harder, E. D. (2021). Opls4: Improving force field accuracy on challenging regimes of chemical space. *Journal of Chemical Theory and Computation*, 17(7), 4291–4300. <https://doi.org/10.1021/acs.jctc.1c00302>
- Maity, A., Sarkar, S., Theeyancheri, L., & Chakrabarti, R. (2020). Choline chloride as a nano-crowder protects hp-36 from urea-induced denaturation: Insights from solvent dynamics and protein-solvent interactions. *ChemPhysChem*, 21(6), 552–567. <https://doi.org/10.1002/cphc.201901078>
- Meersman, F., Atilgan, C., Miles, A. J., Bader, R., Shang, W., Matagne, A., Wallace, B. A., & Koch, M. H. J. (2010). Consistent picture of the reversible thermal unfolding of hen egg-white lysozyme from experiment and molecular dynamics. *Biophysical Journal*, 99(7), 2255–2263. <https://doi.org/10.1016/j.bpj.2010.07.060>
- Monhemi, H., Housaindokht, M. R., Moosavi-Movahedi, A. A., & Bozorgmehr, M. R. (2014). How a protein can remain stable in a solvent with high content of urea: Insights from molecular dynamics simulation of candida antarctica lipase b in urea: Choline chloride deep eutectic solvent. *Physical Chemistry Chemical Physics*, 16(28), 14882–14893. <https://doi.org/10.1039/C4CP00503A>
- Paiva, A., Craveiro, R., Aroso, I., Martins, M., Reis, R. L., & Duarte, A. R. C. (2014). Natural deep eutectic solvents – Solvents for the 21st century. *ACS Sustainable Chemistry & Engineering*, 2(5), 1063–1071. <https://doi.org/10.1021/sc500096j>
- Pal, S., Roy, R., & Paul, S. (2020). Potential of a natural deep eutectic solvent, glyceline, in the thermal stability of the TRP-cage mini-protein. *The Journal of Physical Chemistry. B*, 124(35), 7598–7610. <https://doi.org/10.1021/acs.jpccb.0c03501>
- Parisse, G., Narzi, D., Belviso, B. D., Capriati, V., Caliandro, R., Trotta, M., & Guidoni, L. (2023). Unveiling the influence of hydrated deep eutectic solvents on the dynamics of water-soluble proteins. *The Journal of Physical Chemistry. B*, 127(29), 6487–6499. <https://doi.org/10.1021/acs.jpccb.3c00935>

- Pätzold, M., Siebenhaller, S., Kara, S., Liese, A., Syltatk, C., & Holtmann, D. (2019). Deep eutectic solvents as efficient solvents in biocatalysis. *Trends in Biotechnology*, 37(9), 943–959. <https://doi.org/10.1016/j.tibtech.2019.03.007>
- Plotka-Wasyłka, J., de la Guardia, M., Andruch, V., & Vilková, M. (2020). Deep eutectic solvents vs ionic liquids: Similarities and differences. *Microchemical Journal*, 159, 105539. <https://doi.org/10.1016/j.microc.2020.105539>
- Release, S. (2021). Maestro, Schrodinger, LLC, New York. In *Schrodinger release 2021-1*. Schrodinger, LLC.
- Salehi, H. S., Ramdin, M., Moultos, O. A., & Vlugt, T. J. (2019). Computing solubility parameters of deep eutectic solvents from molecular dynamics simulations. *Fluid Phase Equilibria*, 497, 10–18. <https://doi.org/10.1016/j.fluid.2019.05.022>
- Sanati, A., Malayeri, M. R., Busse, O., & Weigand, J. J. (2021). Inhibition of asphaltene precipitation using hydrophobic deep eutectic solvents and ionic liquid. *Journal of Molecular Liquids*, 334, 116100. <https://doi.org/10.1016/j.molliq.2021.116100>
- Sanchez Fernandez, A., Prevost, S., & Wahlgren, M. (2022). Deep eutectic solvents for the preservation of concentrated proteins: The case of lysozyme in 1:2 choline chloride: Glycerol. *Green Chemistry*, 24(11), 4437–4442. <https://doi.org/10.1039/D1GC04378A>
- Sanchez-Fernandez, A., Basic, M., Xiang, J., Prevost, S., Jackson, A. J., & Dicko, C. (2022). Hydration in deep eutectic solvents induces non monotonic changes in the conformation and stability of proteins. *Journal of the American Chemical Society*, 144(51), 23657–23667. <https://doi.org/10.1021/jacs.2c11190>
- Sanchez-Fernandez, A., Edler, K. J., Arnold, T., Alba Venero, D., & Jackson, A. J. (2017). Protein conformation in pure and hydrated deep eutectic solvents. *Physical Chemistry Chemical Physics*, 19(13), 8667–8670. <https://doi.org/10.1039/C7CP00459A>
- Sarkar, S., Ghosh, S., & Chakrabarti, R. (2017). Ammonium based stabilizers effectively counteract urea-induced denaturation in a small protein: Insights from molecular dynamics simulations. *RSC Advances*, 7(83), 52888–52906. <https://doi.org/10.1039/C7RA10712A>
- Shehata, M., Unlu, A., Sezerman, U., & Timucin, E. (2020). Lipase and water in a deep eutectic solvent: Molecular dynamics and experimental studies of the effects of water-in-deep eutectic solvents on lipase stability. *The Journal of Physical Chemistry. B*, 124(40), 8801–8810. <https://doi.org/10.1021/acs.jpcc.0c07041>
- Silva, N. H. C. S., Vilela, C., Pinto, R. J. B., Martins, M. A., Marrucho, I. M., & Freire, C. S. R. (2018). Tuning lysozyme nanofibers dimensions using deep eutectic solvents for improved reinforcement ability. *International Journal of Biological Macromolecules*, 115, 518–527. <https://doi.org/10.1016/j.ijbiomac.2018.03.150>
- Smith, E. L. (2013). Deep eutectic solvents (DESs) and the metal finishing industry: Where are they now? *Transactions of the IMF*, 91(5), 241–248. <https://doi.org/10.1179/0020296713Z.000000000120>
- Smith, E. L., Abbott, A. P., & Ryder, K. S. (2014). Deep eutectic solvents (DESs) and their applications. *Chemical Reviews*, 114(21), 11060–11082. <https://doi.org/10.1021/cr300162p>
- Smith, P. E., & van Gunsteren, W. F. (1994). Translational and rotational diffusion of proteins. *Journal of Molecular Biology*, 236(2), 629–636. <https://doi.org/10.1006/jmbi.1994.1172>
- Weiz, G., Braun, L., Lopez, R., de María, P. D., & Breccia, J. D. (2016). Enzymatic deglycosylation of flavonoids in deep eutectic solvents aqueous mixtures: Paving the way for sustainable flavonoid chemistry. *Journal of Molecular Catalysis B: Enzymatic*, 130, 70–73. <https://doi.org/10.1016/j.molcatb.2016.04.010>
- Woodley, J. (2019). Accelerating the implementation of biocatalysis in industry. *Applied Microbiology and Biotechnology*, 103(12), 4733–4739. <https://doi.org/10.1007/s00253-019-09796-x>
- Xu, P., Wang, Y., Chen, J., Wei, X., Xu, W., Ni, R., Meng, J., & Zhou, Y. (2019). Development of deep eutectic solvent-based aqueous biphasic system for the extraction of lysozyme. *Talanta*, 202, 1–10. <https://doi.org/10.1016/j.talanta.2019.04.053>
- Yadav, N., & Venkatesu, P. (2022). Current understanding and insights towards protein stabilization and activation in deep eutectic solvents as sustainable solvent media. *Physical Chemistry Chemical Physics*, 24(22), 13474–13509. <https://doi.org/10.1039/D2CP00084A>
- Yokomizo, T., Higo, J., & Nakasako, M. (2005). Patterns and networks of hydrogen-bonds in the hydration structure of human lysozyme. *Chemical Physics Letters*, 410(1–3), 31–35. <https://doi.org/10.1016/j.cplett.2005.04.072>
- Zhang, J.-Z., Peng, X.-Y., Liu, S., Jiang, B.-P., Ji, S.-C., & Shen, X.-C. (2019). The persistence length of semiflexible polymers in lattice Monte Carlo simulations. *Polymers*, 11(2), 295. <https://doi.org/10.3390/polym11020295>
- Zhang, Q., De Oliveira Vigier, K., Royer, S., & Jérôme, F. (2012). Deep eutectic solvents: Syntheses properties and applications. *Chemical Society Reviews*, 41(21), 7108–7146. <https://doi.org/10.1039/C2CS35178A>